Statistics of Fourier modes in a turbulent flow

Cédric Brun and Alain Pumir
Institut Non Linéaire de Nice, CNRS, 1361 Route des Lucioles, F-06560, Valbonne, France
(Received 26 October 2000; published 25 April 2001)

Fourier series are often used to discuss the properties of a homogeneous turbulent field. We investigate the statistics of Fourier modes of the turbulent velocity field and of a passive scalar. The statistics of individual Fourier modes is known to be Gaussian when the size of the system L is much larger that the integral (correlation) size l_0. The case where the integral size is of the order of the system size $L \sim l_0$, is studied by direct numerical simulations in the range $20 \lesssim R_\lambda \lesssim 80$. At a given R_λ, we find that the probabilities of large fluctuations become larger when the wave number increases, in qualitative agreement with the notion of intermittency. As the Reynolds number increases, however, the probability density functions become closer to Gaussian, in sharp contrast with the behavior of velocity increments. We also show that in a simple model of cascade, the Fourier series decomposition is not appropriate to capture intermittency effects. Last, we discuss other issues related to our results.

DOI: 10.1103/PhysRevE.63.056313 PACS number(s): 47.27.Ak, 47.27.Gs

I. INTRODUCTION

Fully developed turbulence in fluids exhibits a number of unusual properties [1–3]. Despite much theoretical effort, small-scale intermittency remains a challenging problem. One of the main observations is that, as one considers smaller and smaller scales in the flow, the probability distribution functions (PDF's) of the velocity increments, denoted here as $\Delta u(r) \equiv [u(r) - u(0)]$, develop wider and wider tails. Equivalently the dimensionless moments, $S_n(r) \equiv \langle [\Delta u(r)]^{2n} \rangle / \langle [\Delta u(r)]^2 \rangle^n$, grow when r decreases [4]. An even more pronounced effect is found in the related problem of a passive scalar mixed by a turbulent flow [5].

These observations are at odds with the results of the Kolmogorov 1941 theory [6] (in short, K41), which would predict that the $S_n(r)$ are all independent of r in the inertial range of scales. A number of phenomenological models have been proposed to describe this effect [1–3]. So far, analytic calculations have been possible only in simplified models of passive scalar advection [7–9].

Experimentally, most of the work has been devoted to the velocity scalar differences and its moments. One may however ask more general questions about the N-point correlation function: $\langle u(\vec{x}_1) u(\vec{x}_2) \ldots u(\vec{x}_N) \rangle$, or about its Fourier analog: $\langle \hat{u}(\vec{q}_1) \hat{u}(\vec{q}_2) \ldots \hat{u}(\vec{q}_N) \rangle$ (with the condition that $\vec{q}_1 + \vec{q}_2 + \cdots + \vec{q}_N = \vec{0}$ when the flow is homogeneous). Due to the recent development of ultrasound scattering experiments [10], it is now possible to directly obtain information on the Fourier components of the vorticity field and of the temperature field, hence on a passive scalar field.

Early closure attempts of the Navier-Stokes equations were formulated in Fourier space [11,12], since it is usual to use the Fourier representation to investigate correlation functions when the problem is homogeneous. Indeed the Navier-Stokes equations can be readily written in terms of the Fourier amplitudes $\hat{\vec{u}}(\vec{k},t)$. Amplitudes $\hat{\vec{u}}(\vec{k},t)$ play the role of elementary dynamical variables of a kind of infinite-body problem. Coupling among them results from the nonlinearity of the Navier-Stokes equations through a complex web of triadic interactions. Due to the infinite number of modes in interaction added to complex geometry or incompressibility constraints in k space, it seems rather hard to analyze their statistical properties. Even in a strongly decimated approximation, such as the shell models of turbulence, basic difficulties remain, namely the presence of both dissipation and strong nonlinearity. In fact, it is only in the inviscid and unforced case that success in using the $\hat{\vec{u}}(\vec{k},t)$ variables has been achieved to describe the energy equipartition state (Boltzmann-Gibbs equilibrium for the cutoff Euler dynamics) [13,14].

The first and easiest step is to investigate the *equal-time univariate* statistics of the Fourier amplitudes. It is natural to argue that the Fourier modes, which result from some volume average, are not well suited for describing intermittency, which is a spotty phenomenon. However, this argument does not hold in the far-dissipation range where strong intermittency of the Fourier modes is expected, see below. As a consequence of the lack of space localization of the Fourier representation, individual Fourier modes suffer from a spatial central limit effect: for a homogeneous velocity field with finite correlation length l_0 confined in a cubic box of size L with periodic boundary conditions, it is well known that the univariate distribution of individual inertial Fourier component should be asymptotically normal in the limit $l_0/L \to 0$, even if the velocity field is highly intermittent in physical space [15]. It is in fact a particular case of the central limit theorem as it applies to weighted integrals of random fields (see Ref. [16], and also Ref. [17] in the case of cosmological density fields). To illustrate this point, we use a one-dimensional (1D) notation for the sake of simplicity. Let us expand the velocity field in a Fourier series

$$u(x,t) = \sum_k \hat{u}(k,t) e^{ik \cdot x}. \tag{1.1}$$

Then $\hat{u}(k,t)$ reads

$$\hat{u}(k,t) = \frac{1}{L} \int e^{-ik \cdot x} u(x,t) dx. \tag{1.2}$$

Consider a Fourier mode $\hat{u}(k,t)$ with $k>2\pi/l_0$. For L sufficiently large, it is possible to divide the segment of size L into subsegments of a size multiple of $2\pi/k$ and large compared to l_0. Then using Eq. (1.2), $\hat{u}(k,t)$ can be rewritten as a sum of very many weakly correlated and identically distributed terms. For an energy cascade of a fixed size, assuming the velocity field to satisfy certain mixing conditions (roughly speaking, the correlations are supposed to decrease fast enough), the central limit theorem can thus be applied to the real or imaginary part of any inertial or dissipative Fourier component (more precisely, it applies to the joint statistics of the real and imaginary part properly renormalized). Nevertheless, because of intermittency, it is hard to estimate how the convergence to Gaussian statistics depends on the wave number.

This trivial central limit effect seems in fact independent of the detailed dynamics [18]. Hence, when the correlation length is of the order of the domain extension, like in direct numerical simulations (DNS) or in some laboratory experiments, one may expect intermittency corrections for individual Fourier components. The purpose of this paper is to investigate this issue, and in particular to compare with recent experimental results [10]. Naively, one would expect that the statistical properties of $\hat{\vec{u}}(\vec{k},t)$ are similar to the properties of $\Delta u(r)$ for $r\sim 1/k$. A recent study seems to support this claim [19]. Our own numerical results are in sharp contrast with this expectation, as we will explain in Sec. II. In qualitative agreement with the experimental results [10], we found very little variation of the statistical properties of the $\hat{\vec{u}}(\vec{k},t)$ through inertial scales. In Sec. III, we consider an intermittent velocity field resulting from a simple wavelet cascade, and show that the statistics of Fourier modes is almost insensitive to intermittency in the sense that the distribution of $\hat{u}(k)$ depends very weakly on k. The last section is devoted to discussion. There we address the question of sweeping effects as far as Fourier modes are concerned, and also the link with some simplified dynamical models of turbulence such as the so-called shell models or tree models, and last, the possiblity of looking simultaneously at several wave numbers to take into account weak coupling between Fourier modes and to measure intermittency.

II. NAVIER-STOKES AND PASSIVE SCALAR DYNAMICS

A. Numerical methods

We have simulated numerically the incompressible Navier-Stokes equations along with the passive scalar equation:

$$\partial_t\vec{u}+(\vec{u}\cdot\vec{\nabla})\vec{u}=-\vec{\nabla}p+\nu\nabla^2\vec{u}, \tag{2.1}$$

$$\vec{\nabla}\cdot\vec{u}=0, \tag{2.2}$$

$$\partial_t\theta+(\vec{u}\cdot\vec{\nabla})\theta=\kappa\nabla^2\theta. \tag{2.3}$$

The spatial domain is a cubic box with a periodicity length equal to 2π. Our code has been described elsewhere [20], and we briefly recall its main features. We use a pseudospectral, fully dealiased code. The solution is time stepped by a leap-frog algorithm, second order in time. A homogeneous, isotropic, steady state is obtained by imposing a conservative dynamics in the low wave-number modes ($k\leqslant 1.5$). We also perform DNS of incompressible Navier-Stokes equations with hyperviscosity $(-1)^{h+1}\nu\nabla^{2h}$ ($h=2$ and $h=8$).

The velocity and scalar field being homogeneous, the statistics of Fourier components is phase invariant. In particular, the real and imaginary parts of these quantities have the same distribution; their odd order cross correlation are zero [$\langle \mathrm{Re}(\cdot)^p\mathrm{Im}(\cdot)^q\rangle=0$ if $p+q$ odd], but the real and imaginary parts are not strictly independent (indeed we expect their statistical coupling to be very weak, see Sec. IV C). Because of incompressibility, $\hat{\vec{u}}(\vec{k})$ may be represented in terms of its projections on two units vectors $\hat{e}^+(\vec{k})$ and $\hat{e}^-(\vec{k})$ such that $(\vec{k},\hat{e}^+(\vec{k}),\hat{e}^-(\vec{k}))$ forms an orthogonal basis. This decomposition allows us to carry out statistics on $\hat{u}^\pm(\vec{k})\equiv\hat{\vec{u}}(\vec{k})\cdot\hat{e}^\pm(\vec{k})$. Because of isotropy, $\hat{u}^+(\vec{k})$ and $\hat{u}^-(\vec{k})$ have the same statistics. Using again isotropy, the PDF's of the real and imaginary parts of $\hat{\theta}(\vec{k})$ and $\hat{u}^\pm(\vec{k})$ were accumulated over thin shells of wave vectors $\vec{k}$, where $K-1/2\leqslant|\vec{k}|\leqslant K+1/2$ for a number of values of K. We consider also the statistics of $|\hat{\theta}(\vec{k})|$ and $|\hat{\vec{u}}(\vec{k})|$ to take into account the coupling between components and between real and imaginary parts. We estimated the various PDF's by a histogram binning procedure. The statistics were accumulated over a sampling time T_s. In terms of the (large scale) eddy turnover time $T_e\equiv l_0/\langle u_x^2\rangle^{1/2}$, the sampling time T_s was always larger than $13T_e$. Even so, it should be noted that, especially for low wave numbers, despite accumulation in thin k shells, much less data are collected in the statistics of a Fourier component than in the statistics of differences in real space, which are computed at each grid point.

For our runs with Newtonian dissipation, the Reynolds number, based on the Taylor scale, λ $\{\lambda\equiv[\langle u_x^2\rangle/\langle(\partial_x u_x)^2\rangle]^{1/2}\}$, was varied in the range $20\leqslant R_\lambda\leqslant 80$; the Prandtl number is kept unity.

We used hyperviscous DNS in order to qualitatively discriminate between inertial and dissipative dynamics. The numerical integration requires very little modifications. For hyperviscous runs, the Reynolds number is not well defined (see however Ref. [21] for a proposal). In Table I, we give the hyperviscous index h and the wave number k_d corresponding to the maximum of the dissipation spectrum.

To measure the numerical resolution of the small scales in Newtonian runs, one usually computes the product $k_{max}\eta$, where k_{max} is the largest wave number and $\eta\equiv(\nu^3/\varepsilon)^{1/4}$ is the Kolmogorov scale, ε being the rate of dissipation of kinetic energy per unit mass. We maintained $k_{max}\eta\gtrsim 1.5$. By analogy, one may equilibrate a turnover time with a hyperviscous dissipation time to define the analog of the Kolmogorov scale $\eta_h\equiv(\nu^3/\varepsilon)^{1/2(3h-1)}$ depending on the power of the hyperviscous dissipation. However, the corresponding values of the product $k_{max}\eta_h$ have not been documented in the literature to estimate the resolution of the small scales.

TABLE I. A list of our NS runs with parameters.

Run no.	R_λ	Pr	N	h	k_d	l_0^u	l_0^θ	$k_{max}\eta$	T_s/T_e
NS1	20.0	1	40	1	2	1.7	1.1	2.3	1507.0
NS2	40.0	1	64	1	4	1.5	1.0	1.8	103.0
NS3	80.0	1	128	1	9	1.3	1.0	1.5	13.0
NS4			64	2	13	1.2			53.0
NS5			64	8	25	1.2			50.0

Here, we insisted that the value of the dissipation spectrum, $k^{2h}E(k)$, for the largest available wave number in the simulation, was less than $\sim 7\%$ of its maximum value.

We stress that the forcing scheme has been unchanged in our various runs. We computed the integral scales of the velocity and scalar field, defined as $l_0^u \equiv (\pi/2)1/\langle u_x^2\rangle \int k^{-1}E_u(k)\,dk$ and $l_0^\theta \equiv \pi(1/\langle\theta^2\rangle)\int k^{-1}E_\theta(k)\,dk$. Between our various runs, we get $l_0^u \approx 1.5$ and $l_0^\theta \approx 1.0$. With our box size $L=2\pi$ and because of periodicity, we expect a weak central limit effect on the individual Fourier modes.

Table I shows a list of our runs with the sampling times and parameters that permit us to judge the quality of the resolution.

B. Results at (very) low R_λ

The PDF's of $\mathrm{Re}[\hat\theta(\vec k)]$, $\mathrm{Re}[\hat u^{\pm}(\vec k)]$, in units of their root-mean-square (rms) values are shown in Figs. 1(a) and 1(b), for several values of the wave number K, and $R_\lambda \sim 20$. At $R_\lambda \sim 20$, there is no basis for an inertial range cascade since the velocity and scalar spectra are falling off roughly exponentially, see Fig. 2. Thus, the intermittent behavior of the PDF's seems at first surprising.

In fact, the behavior of the PDF's cannot be related to inertial intermittency but rather to dissipative intermittency [22]. The far-dissipation range has been predicted to display strong intermittency even at low Reynolds numbers; on physical grounds, if the velocity spectrum decreases faster than algebrically, every minute fluctuation of ε should be tremendously amplified as $k\eta \to \infty$ [23]. High-resolution simulation of the dissipation range at $R_\lambda \sim 15$ has confirmed that dissipative intermittency is associated with gentle spatial variation of large-scale structure [24]. Frisch and Morf gave more systematic and generic arguments [25]. From a dynamical point of view, the zero fixed point of the linearized dynamics may also play an important role in the occurence of dissipative bursts [26]. Due to the sharp decay of the velocity spectrum in our simulation at $R_\lambda \sim 20$, even if we do not have a clear dissipation range, we believe that the previous explanation applies.

The arguments referred to above suggest that the intermittency of the $\hat u(k)$ should grow *without limit* as $k\eta \to \infty$, at any finite Reynolds number. The behavior of the Fourier components is therefore different from the behavior of the velocity differences; at finite Reynolds number, when $r \to 0$, all the moments of the distribution of $\Delta u(r)$ are bounded from above by the moments of the distribution of the gradients, which are finite.

C. Results at higher R_λ

In Figs. 1(c)–1(d) and 1(e)–1(f), we present the same study at, respectively, $R_\lambda \sim 40$ and $R_\lambda \sim 80$. As it is the case at $R_\lambda \sim 20$, the Fourier modes of the velocity and scalar fields present the same qualitative behavior. For each Reynolds number, the PDF's of $\mathrm{Re}[\hat\theta(\vec k)]/\langle \mathrm{Re}[\hat\theta(\vec k)]^2\rangle^{1/2}$ and $\mathrm{Re}[\hat u^{\pm}(\vec k)]/\langle \mathrm{Re}[\hat u^{\pm}(\vec k)]^2\rangle^{1/2}$ become wider when the wave number increases. But remarkably, this effect is reduced as the Reynolds numbers is increased. At $R_\lambda \sim 80$, the PDF's are very close to Gaussian; in particular, the widening effect is clearly much weaker than for the velocity differences.

We show in Figs. 3(a)–3(d) the PDF's of $|\hat\theta(\vec k)|/\langle|\hat\theta(\vec k)|^2\rangle^{1/2}$ and $|\hat{\vec u}(\vec k)|/\langle|\hat{\vec u}(\vec k)|^2\rangle^{1/2}$ obtained at $R_\lambda \sim 80$ in semilog and log-log coordinates. As before, a very weak evolution through the scales is observed. Assuming the real and imaginary parts of $\hat\theta(\vec k)$ to be Gaussian and independent, it is straightforward to check that $Z = |\hat\theta(\vec k)|/\langle|\hat\theta(\vec k)|^2\rangle^{1/2}$ should be distributed according to the Rayleigh distribution $P(Z) = 2Z\exp(-Z^2)$ defined for $Z \geqslant 0$. Similarly, with the additional hypothesis of $\hat u^+(k)$ and $\hat u^-(k)$ being independent, $Z = |\hat{\vec u}(\vec k)|/\langle|\hat{\vec u}(\vec k)|^2\rangle^{1/2}$ should be distributed according to the distribution $P(Z) = 8Z^3\exp(-2Z^2)$ defined for $Z \geqslant 0$. The agreement with the two above distributions is only good for very small deviation ($Z \to 0$), see Figs. 3(b) and 3(d). The deviations observed at larger values of Z are related to the deviations from the Gaussian distribution observed at large values of $\mathrm{Re}[\hat\theta(\vec k)]/\langle \mathrm{Re}[\hat\theta(\vec k)]^2\rangle^{1/2}$ and $\mathrm{Re}[\hat u^{\pm}(\vec k)]/\langle \mathrm{Re}[\hat u^{\pm}(\vec k)]^2\rangle^{1/2}$. But there is still a good collapse of the PDF's in the inertial range.

In Ref. [19] and in the case of Navier-Stokes (NS) dynamics, it has been argued on the basis of DNS with a 64^3 resolution that scaling exponents of longitudinal increments and individual Fourier modes, respectively, ζ_p and z_p, should only differ by a linear ''phase-space'' factor: $z_p = \zeta_p + 3p/2$. We already stressed that the statistics of individual Fourier components are always plagued by central limit effect, and thus are very unlikely to be universal, due to the strong influence of the ratio l_0/L. More significantly, the above relation implies that $z_p - p/2z_2 = \zeta_p - p/2\zeta_2$, so the quantities $|\hat{\vec u}(\vec k)|/\langle|\hat{\vec u}(\vec k)|^2\rangle^{1/2}$ [or $\mathrm{Re}[\hat u^{\pm}(k)]/\langle \mathrm{Re}[\hat u^{\pm}(k)]^2\rangle^{1/2}$] and $\Delta u(r)/\langle \Delta u(r)^2\rangle^{1/2}$ should present the same multiscaling. The possibility of determining accurate exponents from our numerics is somewhat questionable. But clearly, at our highest Reynolds number $R_\lambda \sim 80$,

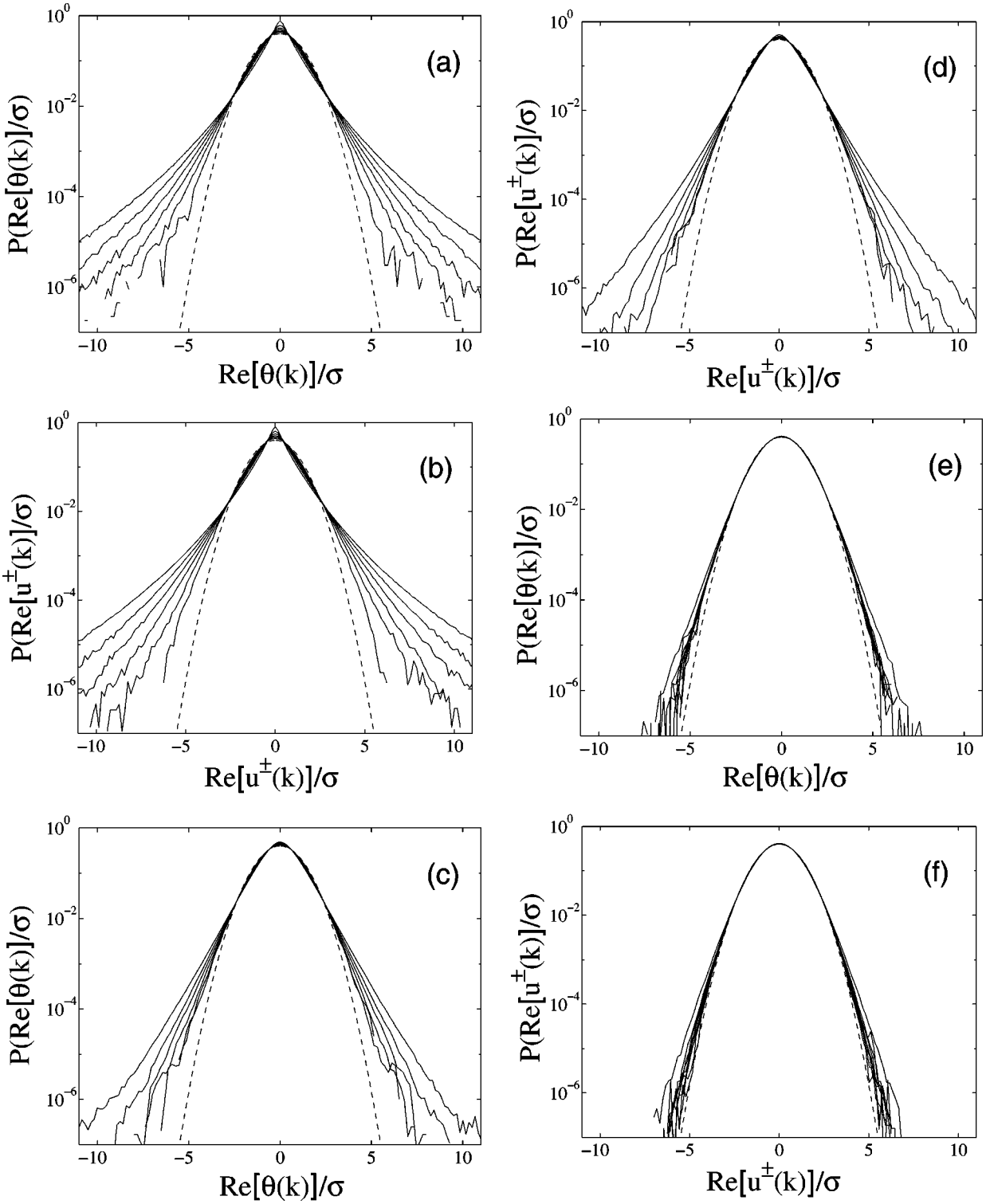

FIG. 1. PDF's of Re$[\hat{\theta}(\vec{k})]$ and Re$[\hat{u}^{\pm}(\vec{k})]$ normalized by their rms value σ. Gaussian PDF of variance unity is shown for comparison in dashed line. (a) and (b): $R_\lambda \sim 20$ (run NS1), $k=3;6;9;12;15;18$. (c) and (d): $R_\lambda \sim 40$ (run NS2), $k=5;10;15;20;25;29$. (e) and (f): $R_\lambda \sim 80$ (run NS3), $k=11;17;23;29;35;41;47;53;59$. The flatness $F_k \equiv \langle \mathrm{Re}[\hat{u}^{\pm}(\vec{k})]^4 \rangle / \langle \mathrm{Re}[\hat{u}^{\pm}(\vec{k})]^2 \rangle^2$ of the mode $k \approx 10$ steadily decreases when the Reynolds number increases; at $R_\lambda \sim 20$, $F_{k=9}=5.0$, at $R_\lambda \sim 40$, $F_{k=10}=3.5$, and at $R_\lambda \sim 80$, $F_{k=11}=3.1$.

the evolution through the scales of our PDF's cannot support the heuristic ansatz proposed in [19].

As our results show a systematic evolution with the Reynolds number, one may wonder what happens at higher Reynolds numbers. The recent ultrasound scattering experiments [10] performed in a turbulent jet in air ($P_r=0.7$), weakly heated so that the temperature fluctuations act as a passive scalar, provide a clue as to what may happen. At $R_\lambda=64$,

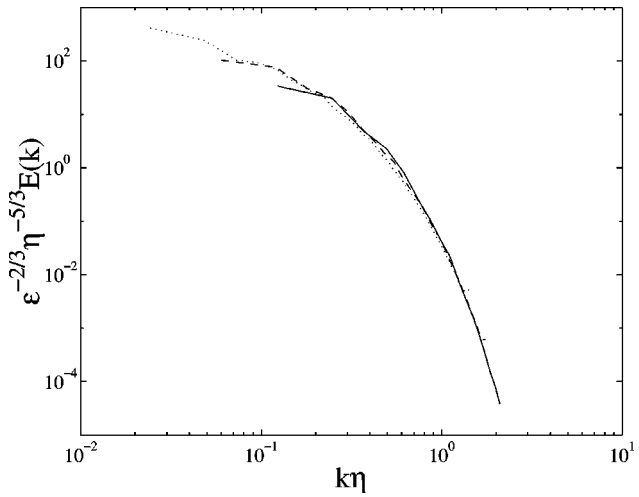

FIG. 2. Velocity spectrum for $R_\lambda \sim 20$ (solid line), ~ 40 (dashed line), ~ 80 (dotted line). The inertial, $k^{-5/3}$ range is essentially absent at the lowest Reynolds number, and gradually builds up as the Reynolds number increases.

statistical measurements of the Fourier components of the temperature field agree qualitatively with our numerical results. We note that this agreement between the numerical and experimental results provides a partial validation of the ultrasound scattering method. In a different configuration and at higher Reynolds numbers [27], the inertial PDF's have a non-Gaussian shape, with seemingly exponential tails. However, once renormalized in rms units, only a slight intermittent evolution is observed in the inertial range. The experimental results should be interpreted with caution, since in the latter configuration, a much poorer spectral resolution is achieved due to the size of the flow [27]. As a result, it is not clear whether the Fourier components are genuinely measured. In any event, we have to distinguish between the *shape* of the PDF's and their *evolution* through scales (scaling). One may naturally suspect the large scales of the flow to be responsible for the form of the PDF's. In our simulations, the forcing modes are very close to Gaussian. We note also that the large scales determine the ratio l_0/L and so the influence of the central limit effect. Independent of the precise shape, the absence of evolution of the PDFs of the Fourier components observed experimentally and numerically at

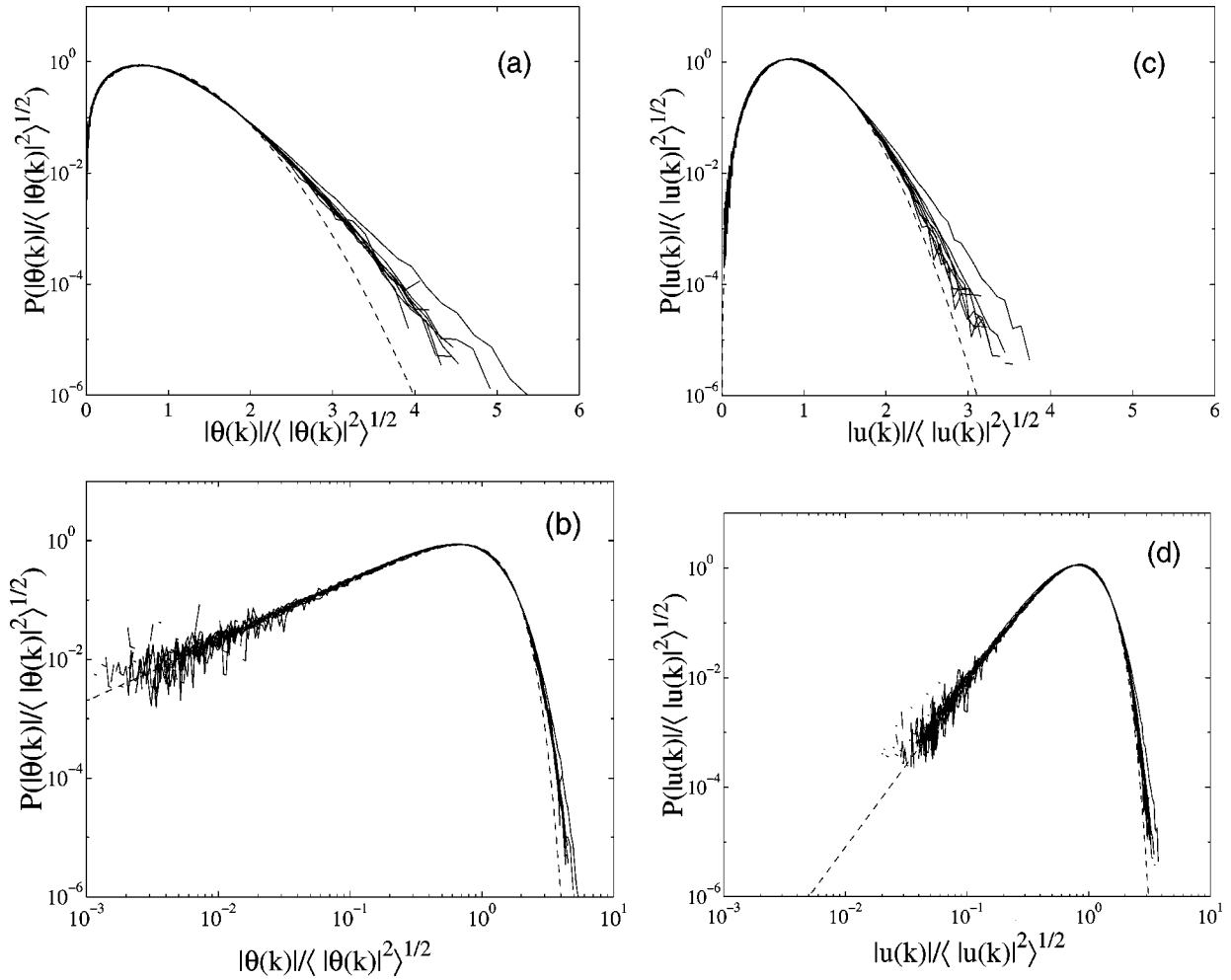

FIG. 3. PDF's of $|\hat{\theta}(\vec{k})|/\langle|\hat{\theta}(\vec{k})|^2\rangle^{1/2}$ and $|\hat{\tilde{u}}(\vec{k})|/\langle|\hat{\tilde{u}}(\vec{k})|^2\rangle^{1/2}$ at $R_\lambda \sim 80$ (run NS3). Wave numbers are $k = 11;17;23;29;35;41;47;53;59$. (a) and (b) PDF $P(Z) = 2Z\exp(-Z^2)$ is shown for comparison in dashed line. (c) and (d) PDF $P(Z) = 8Z^3\exp(-2Z^2)$ is shown for comparison in dashed line.

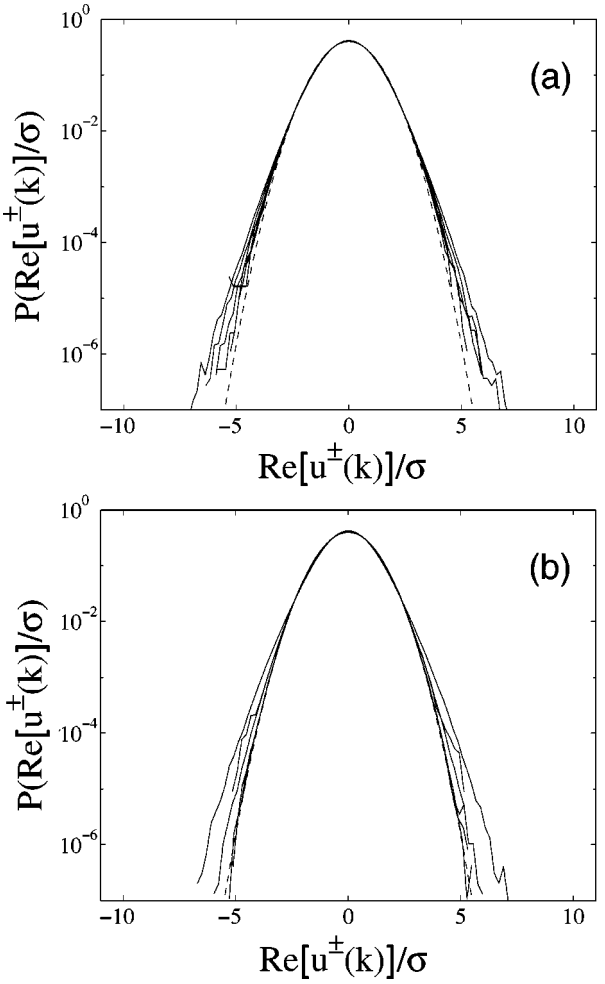

FIG. 4. PDF's of $\mathrm{Re}[\hat{u}^{\pm}(\vec{k})]$ normalized by their rms value σ, for hyperviscous NS runs. Gaussian PDF of variance unity is shown for comparison in dashed line. (a) Hyperviscous index $h=2$ (run NS4), $k=5;10;15;20;25;29$. (b) Hyperviscous index $h=8$ (run NS5). $k=5;10;15;20;25;29$.

our highest available Reynolds numbers is very suggestive.

Due to the limited inertial range available in our simulations, we reconsider the problem with a hyperviscous damping $(-1)^{h+1}\nu\nabla^{2h}$. In Figs. 4(a)–4(b), we present the results of 64^3 hyperviscous runs with $h=2$ and $h=8$. Again we find that the PDF's of $\mathrm{Re}(\hat{u}^{\pm}(\vec{k}))$ are very close to Gaussian, all the way down to the dissipative scale. In particular for $h=8$, it is clearly seen that the PDF's of $\mathrm{Re}(\hat{u}^{\pm}(\vec{k}))$ almost collapse to a Gaussian shape for $k\leqslant 25$. A clear, albeit small deviation can be seen for $k=29>k_d=25$.

Our numerical results demonstrate that as long as the nonlinear term dominates, the distribution of Fourier modes is essentially Gaussian. As soon as viscous processes become important, the complex interplay between nonlinearity and dissipation results in larger fluctuations of the Fourier modes.

III. LACK OF INTERMITTENCY OF FOURIER MODES IN A SIMPLE MODEL OF CASCADE

In this section, we consider a simple 1D wavelet cascade that allows us to generate multiaffine velocity fields [28]. We demonstrate that the Fourier transform of the synthetic velocity field does not exhibit any particular intermittency, as a result of a ''hidden'' spatial central limit effect. We shall discuss the validity of this approach. We note that similar computations have already been done for the wavelet analysis of a probabilistic wavelet cascade [29].

Following Benzi *et al.* [28], we consider $u(x)$ given by the following wavelet decomposition

$$u(x)\equiv\sum_{n=-\infty}^{+\infty}\sum_{j=-\infty}^{+\infty}\alpha_{n,j}\Psi_{n,j}(x), \tag{3.1}$$

where

$$\Psi_{n,j}(x)=2^{n/2}\Psi_{0,0}(2^n x-j), \tag{3.2}$$

and $\Psi_{0,0}$ is the mother wavelet, with zero mean, localized both in space and scale. For the discrete case with 2^N points $x_s=s(1/2^N)$ in the interval $[0,1]$, we have

$$u(x_s)\equiv\sum_{n=0}^{N-1}\sum_{j=0}^{2^n-1}\alpha_{n,j}\Psi_{n,j}(x_s). \tag{3.3}$$

The coefficients $\alpha_{n,j}$ are defined using the following multiplicative process:

$$\alpha_{0,0}=1, \tag{3.4}$$

$$\alpha_{n+1,2j}=\epsilon_{n+1,2j}W_{n+1,2j}\alpha_{n,j}, \tag{3.5}$$

$$\alpha_{n+1,2j+1}=\epsilon_{n+1,2j+1}W_{n+1,2j+1}\alpha_{n,j}. \tag{3.6}$$

The $\epsilon_{n,j}$ are independent random variables equal ± 1 with probability 1/2 (this simplifying choice will be discussed later). The random multipliers $W_{n,j}$ are independent positive variables, with the same distribution $P(W)$.

It is easy to show that $\langle|\alpha_{n,j}|^p\rangle=\langle W^p\rangle^n$, where the average is performed over the ensemble of the realizations of the multiplicative process. Denoting $\zeta_p\equiv-\log_2\langle W^p\rangle$, we have $\langle|\alpha_{n,.}|^p\rangle=2^{-\zeta_p}\langle|\alpha_{n-1,.}|^p\rangle=2^{-n\zeta_p}$. The scaling exponents ζ_p are chosen to give intermittent multiscaling. Note that in this model, $L=1$ is fixed, and $l_0\sim L$ since there is only a single mother eddy.

Taking the discrete Fourier transform of Eq. (3.3), $\hat{u}(k)$ reads

$$\hat{u}(k)=\sum_{n=0}^{N-1}\sum_{j=0}^{2^n-1}\alpha_{n,j}\hat{\Psi}_{n,j}(k). \tag{3.7}$$

We remind that the $\hat{\Psi}_{n,j}(k)$ are localized in k space. Moreover, at fixed n, the $\hat{\Psi}_{n,j}(k)$ differ only by a (deterministic) phase term $[\hat{\Psi}_{n,j}(k)=e^{-ikj/2^n}\hat{\Psi}_{n,0}(k)]$. Therefore, we further simplify by considering only

$$S_n\equiv\sum_{j=0}^{2^n-1}\alpha_{n,j}. \tag{3.8}$$

We expect $\hat{u}(k)$ and S_n to have the same relative scaling.

We note that the sum in Eq. (3.8) is over 2^n terms. If one intends to invoke the central limit theorem for S_n (properly renormalized), the crucial point is the spatial correlations of the $\alpha_{n,j}$. For the multiplicative process considered here, one may expect the spatial correlations of the $\alpha_{n,j}$ to decrease only slowly through the scales, while the $\alpha_{n,j}$ become more intermittent. So there is no hope for a direct application of the central limit theorem as $n\to\infty$. Instead, we have to compute the moments of S_n, which involve naturally the spatial correlations of the $\alpha_{n,j}$. Therefore, we stress that the relevance of this approach relies on the capacity of the models (3.4)–(3.6) to describe the spatial correlations of the $\alpha_{n,j}$ for a 1D spatial section in true 3D turbulence (note that we deal here with 1D Fourier transform). Experimental tests have been made in Ref. [30] for the space-scale correlations $\langle \omega_{n_1,j_1}\omega_{n_2,j_2}\rangle$, where $\omega_{n,j}\equiv \frac{1}{2}\ln \alpha_{n,j}^2 - \langle \frac{1}{2}\ln \alpha_{n,j}^2\rangle$. A qualitative agreement has been found with the models (3.4)–(3.6), with some additional features (a better agreement is obtained for a nonscale-invariant cascade, see Ref. [30]). Unfortunately the previous test does not probe the space-scale phase correlations of the wavelet coefficients, i.e. the $\alpha_{n,j}/|\alpha_{n,j}|$ correlations. Though the sign of a wavelet coefficient is function of the wavelet basis functions and oscillates strongly with the spatial position, such correlations have physical meaning and are involved in the $\alpha_{n,j}$ correlations. In our simple model, the $\alpha_{n,j}/|\alpha_{n,j}|$ are linked to the $\epsilon_{n,j}$ product of the ancestors, the $\epsilon_{n,j}$ being random independent multipliers equal to ± 1 with probability 1/2.

In the following, we will focus on the flatness of S_n to estimate the intermittency of $\hat{u}(k)$. For $n\geqslant 1$, observe that $\langle S_n\rangle = 0$ since $\langle \alpha_{n,j}\rangle = 0$. It is easy to obtain the second moment of S_n:

$$\langle S_n^2\rangle = \sum_j \langle \alpha_{n,j}^2\rangle + \sum_{j_1\neq j_2}\langle \alpha_{n,j_1}\alpha_{n,j_2}\rangle \tag{3.9}$$

$$= 2^n\langle \alpha_{n,.}^2\rangle + \sum_{j_1\neq j_2}\langle \epsilon_{n,j_1}\rangle\langle W_{n,j_1}\rangle\langle \epsilon_{n,j_2}\rangle\langle W_{n,j_2}\rangle \times\langle \alpha_{n-1,[1/2\,j_1]}\alpha_{n-1,[1/2\,j_2]}\rangle, \tag{3.10}$$

where $[x]$ denotes the integer part of $x\geqslant 0$. As $\langle \epsilon_{n,j}\rangle = 0$, nondiagonal terms disappear:

$$\langle S_n^2\rangle = 2^n\langle \alpha_{n,.}^2\rangle. \tag{3.11}$$

Similar computations for the fourth moment of S_n give

$$\langle S_n^4\rangle = 2^n\langle \alpha_{n,.}^4\rangle + 3\sum_{j_1\neq j_2}\langle \alpha_{n,j_1}^2\alpha_{n,j_2}^2\rangle. \tag{3.12}$$

Then, we obtain the flatness of S_n

$$\frac{\langle S_n^4\rangle}{\langle S_n^2\rangle^2} = \frac{1}{2^n}\frac{\langle \alpha_{n,.}^4\rangle}{\langle \alpha_{n,.}^2\rangle^2} + \frac{3}{2^{2n}}\sum_{j_1\neq j_2}\frac{\langle \alpha_{n,j_1}^2\alpha_{n,j_2}^2\rangle}{\langle \alpha_{n,.}^2\rangle^2}. \tag{3.13}$$

To take into account the correlations among the $\alpha_{n,j}^2$ terms, we introduce

$$K_{j_1,j_2}^n \equiv \frac{\langle \alpha_{n,j_1}^2\alpha_{n,j_2}^2\rangle - \langle \alpha_{n,.}^2\rangle^2}{\langle \alpha_{n,.}^4\rangle - \langle \alpha_{n,.}^2\rangle^2} > 0. \tag{3.14}$$

Using K_{j_1,j_2}^n, Eq. (3.13) can be rewritten as follows:

$$\frac{\langle S_n^4\rangle}{\langle S_n^2\rangle^2} = 3 + \frac{1}{2^n}\frac{\langle \alpha_{n,.}^4\rangle - 3\langle \alpha_{n,.}^2\rangle^2}{\langle \alpha_{n,.}^2\rangle^2} + \frac{3}{2^{2n}}\sum_{j_1\neq j_2}K_{j_1,j_2}^n\frac{\langle \alpha_{n,.}^4\rangle - \langle \alpha_{n,.}^2\rangle^2}{\langle \alpha_{n,.}^2\rangle^2}. \tag{3.15}$$

The second term of the right-hand side of Eq. (3.15) corresponds to the case of independent $\alpha_{n,j}$ (with respect to the spatial j index). The 2^n number of terms in the sum of S_n competes with the increased intermittency of the $\alpha_{n,j}$ as $n\to\infty$. Assuming $0<2\zeta_2-\zeta_4<1$, we get

$$\frac{1}{2^n}\frac{\langle \alpha_{n,.}^4\rangle - 3\langle \alpha_{n,.}^2\rangle^2}{\langle \alpha_{n,.}^2\rangle^2} = \frac{2^{(2\zeta_2-\zeta_4)n}-3}{2^n} \sim 2^{(2\zeta_2-\zeta_4-1)n}\to 0 \quad \text{as} \quad n\to\infty. \tag{3.16}$$

The evaluation of the third term of Eq. (3.15) is more delicate. We observe that $0<K_{j_1,j_2}^n<1$ and $K_{j_1,j_2}^n = K_{j_2,j_1}^n$. But the multivariate statistics of the $\alpha_{n,j}$ is not homogeneous in its spatial j index, and we may have $K_{j_1,j_2}^n \neq K_{j_1+s,j_2+s}^n$. Nevertheless, one may show that $K_{j_1,j_2}^n \leqslant K_{0,j_2-j_1}^n$ for $j_2 \geqslant j_1$. This allows us to obtain the following inequalities:

$$\sum_{j_1\neq j_2}K_{j_1,j_2}^n = 2\sum_{j_1<j_2}K_{j_1,j_2}^n \leqslant 2\sum_{j_1<j_2}K_{0,j_2-j_1} \leqslant 2/2^n\sum_{j=1}^{2^n-1}K_{0,j}. \tag{3.17}$$

Denoting $(\hat{n},\hat{j})$ the first common ancestor of (n,j_1) and (n,j_2), K_{j_1,j_2}^n takes the form

$$K_{j_1,j_2}^n = \frac{\langle W^2\rangle^{2(n-\hat{n})}\langle \alpha_{\hat{n},\hat{j}}^4\rangle - \langle W^2\rangle^{2(n-\hat{n})}\langle \alpha_{\hat{n},\hat{j}}^2\rangle^2}{\langle W^4\rangle^{n-\hat{n}}\langle \alpha_{\hat{n},\hat{j}}^4\rangle - \langle W^2\rangle^{2(n-\hat{n})}\langle \alpha_{\hat{n},\hat{j}}^2\rangle^2} \tag{3.18}$$

$$= \frac{\langle \alpha_{\hat{n},\hat{j}}^4\rangle/\langle \alpha_{\hat{n},\hat{j}}^2\rangle^2 - 1}{(\langle W^4\rangle/\langle W^2\rangle^2)^{n-\hat{n}}\langle \alpha_{\hat{n},\hat{j}}^4\rangle/\langle \alpha_{\hat{n},\hat{j}}^2\rangle^2 - 1} \tag{3.19}$$

$$= \frac{2^{(2\zeta_2-\zeta_4)\hat{n}}-1}{2^{(2\zeta_2-\zeta_4)n}-1}. \tag{3.20}$$

Therefore, at fixed n, K_{j_1,j_2}^n depends only on the level $\hat{n}$ of the first common ancestor of (n,j_1) and (n,j_2). Using Eq. (3.20), we evaluate $\Sigma_{j=1}^{2^n-1}K_{0,j}^n$

$$\sum_{j=1}^{2^n-1} K_{0,j}^n = \frac{1}{2^{(2\zeta_2-\zeta_4)n}-1} \sum_{q=0}^{n-1} (2^{q(2\zeta_2-\zeta_4)}-1)\times 2^{n-1-q} \tag{3.21}$$

$$= \frac{2^{n-1}}{2^{(2\zeta_2-\zeta_4)n}-1}\left(\frac{1-2^{(2\zeta_2-\zeta_4-1)n}}{1-2^{(2\zeta_2-\zeta_4-1)}} - \frac{1-2^{-n}}{1-1/2}\right). \tag{3.22}$$

Thus, the following bound holds for the third term of Eq. (3.15)

$$0 < \frac{3}{2^{2n}} \sum_{j_1\neq j_2} K_{j_1,j_2}^n \frac{\langle \alpha_{n,.}^4\rangle - \langle \alpha_{n,.}^2\rangle^2}{\langle \alpha_{n,.}^2\rangle^2}$$

$$\leqslant \frac{6}{2^n}\frac{2^{n-1}}{2^{(2\zeta_2-\zeta_4)n}-1}\left(\frac{1-2^{(2\zeta_2-\zeta_4-1)n}}{1-2^{(2\zeta_2-\zeta_4-1)}} - \frac{1-2^{-n}}{1-1/2}\right)\frac{\langle \alpha_{n,.}^4\rangle - \langle \alpha_{n,.}^2\rangle^2}{\langle \alpha_{n,.}^2\rangle^2} \tag{3.23}$$

$$\leqslant \frac{6}{2^n}\frac{2^{n-1}}{2^{(2\zeta_2-\zeta_4)n}-1} \times\left(\frac{1-2^{(2\zeta_2-\zeta_4-1)n}}{1-2^{(2\zeta_2-\zeta_4-1)}} - \frac{1-2^{-n}}{1-1/2}\right) \times (2^{(2\zeta_2-\zeta_4)n}-1) \tag{3.24}$$

$$= \mathcal{O}(1) \quad \text{as} \quad n\to\infty. \tag{3.25}$$

Finally, under the hypothesis $0<2\zeta_2-\zeta_4<1$, we get for the flatness of S_n

$$\frac{\langle S_n^4\rangle}{\langle S_n^2\rangle^2} = 3+\mathcal{O}(1) \quad \text{as} \quad n\to\infty. \tag{3.26}$$

Clearly, for such a cascade, a limited intermittency of the individual Fourier modes is expected as $n\to\infty$.

The previous $\epsilon_{n,j}$ play the role of an approximate random-phase for the ''eddies'' $\alpha_{n,j}$, which leads to important simplifications. In the following, we consider the opposite (also unphysical) case $\epsilon_{n,j}\equiv+1$. Since now $\langle\alpha_{n,j}\rangle>0$, we introduce the centered variables $\alpha'_{n,j}\equiv\alpha_{n,j}-\langle\alpha_{n,j}\rangle$ and $S'_n\equiv S_n-\langle S_n\rangle=\Sigma_j\alpha'_{n,j}$. We compute the second and fourth moment of S'_n:

$$\langle S_n'^2\rangle = 2^n\langle \alpha_{n,.}'^2\rangle + \sum_{j_1\neq j_2}\langle \alpha'_{n,j_1}\alpha'_{n,j_2}\rangle, \tag{3.27}$$

$$\langle S_n'^4\rangle = 2^n\langle \alpha_{n,.}'^4\rangle + 3\sum_{j_1\neq j_2}\langle \alpha_{n,j_1}'^2\alpha_{n,j_2}'^2\rangle + 4\sum_{j_1\neq j_2}\langle \alpha_{n,j_1}'^3\alpha'_{n,j_2}\rangle + \sum_{\substack{j_1,j_2,j_3,j_4\\ \mathcal{N}\{j_1,j_2,j_3,j_4\}\geqslant 3}}\langle \alpha'_{n,j_1}\alpha'_{n,j_2}\alpha'_{n,j_3}\alpha'_{n,j_4}\rangle. \tag{3.28}$$

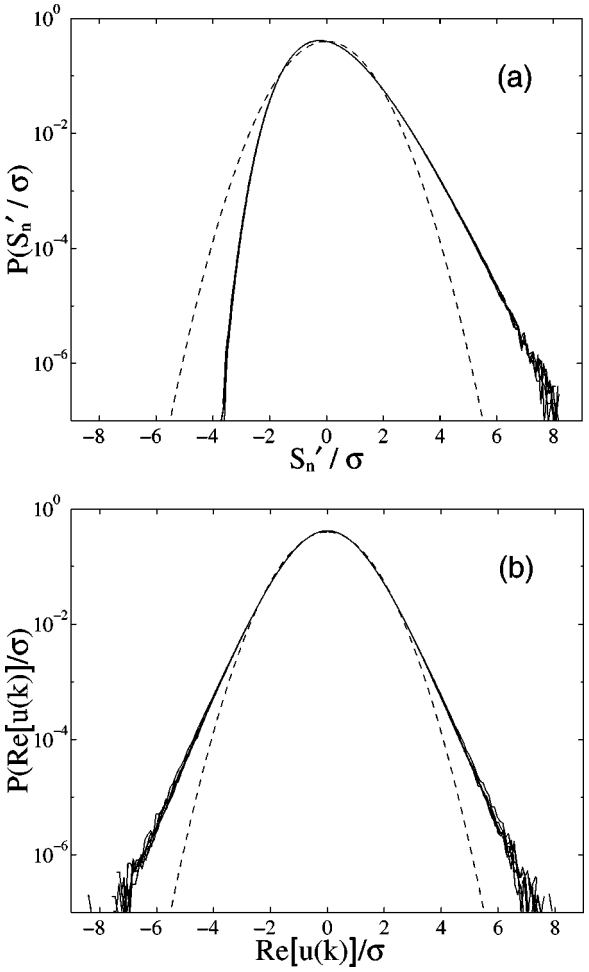

FIG. 5. PDF's of S'_n and $\mathrm{Re}[\hat{u}(\vec{k})]$ normalized by their rms values σ for the multiplicative cascade of Sec. III. Gaussian PDF of variance unity is shown for comparison in dashed line. (a) n=4, . . . ,9. (b) $k=11\times 2^n$, $n=0,\ldots,5$.

The sum in the last term of Eq. (3.28) is over sets containing more than three different indices. In the last term of Eq. (3.28) the sum is over $\sim n^4$ terms instead of $\sim n^2$ terms for the two previous sums. Therefore, the asymptotic behavior of $\langle S_n'^4\rangle/\langle S_n'^2\rangle^2$ is not obvious. Since the last term of Eq. (3.28) is not easy to evaluate analytically, we perform numerical simulations. The distribution of $\log_2(W)$ is taken as a Gaussian with mean $m=-0.4-1/2$ and variance $\sigma^2=0.038$, in order to mimic the multiscaling of $\Delta u(r)$ in true turbulence. We took 2^N points with $N=10$, which enabled us to carry out 10^8 realizations of the multiplicative process. To have access to $u(x)$ from the coeffcients $\alpha_{n,j}$, we used the discrete wavelet transform from [31] (pyramidal algorithm [32]). We chose the 20-tap wavelet of Daubechies [33], which is an orthonormal periodic wavelet basis. Then we obtained the $\hat{u}(k)$ by a simple fast Fourier transform. In Fig. 5(a), we show the PDF's of $S'_n/\langle S_n'^2\rangle^{1/2}$ for $n=4,\ldots,9$. We present the same results in Fig. 5(b) for $\mathrm{Re}(\hat{u}(k))$ with $k=11\times 2^n$ and $n=0,\ldots,5$ (this choice of k corresponds approximately to the maximum of the spectral supports of the $\Psi_{n,j}(x)$, which eliminates spectral overlaps). In the two cases, it is hard to see any reliable evolution through the

scales. The shape difference between the PDF's of S_n' and $\mathrm{Re}(\hat{u}(k))$ is due to the phase factors of the $\hat{\Psi}_{n,j}(k)$. These numerical results demonstrate that, even in the absence of a spatial phase decorrelation in the multiplicative process, the intermittency of the $\hat{u}(k)$ is reduced (though we cannot make any asymptotic statement).

We believe that despite its caricatural simplicity, the simple model we considered sheds some light on the basic mechanism, which reduces the intermittency of the individual Fourier modes. The main finding is that the decrease of spatial correlations with the step of the cascade, albeit small, competes with the increasing intermittency through the scales to give rise to a reduced intermittency for the $\hat{u}(k)$ *via* a kind of spatial central limit effect. The previous model has the advantage to make possible some easy analytical and numerical investigation. But we do not expect our qualitative conclusion to depend on the existence of an exact multiplicative cascade or on the space dimension. Additionaly we considered the 1D Burgers model, which is a well-known case of extreme intermittency: DNS with a δ-function correlated in time forcing at the largest scales gave us again very weak intermittency for the inertial $\hat{u}(k)$ (but with sub-Gaussian statistics, results not shown). Finally, we point out that in true turbulent dynamics, we expect the above-mentioned decorrelation process through the scales to be only an inertial feature. The strong dissipative synchronization observed in numerical simulation of tree models [34] comfort us in this idea. Also such a breakdown of the decorrelation process in the dissipation range would be compatible with the dissipative intermittency of the $\hat{u}(k)$ as $k\eta \to \infty$.

IV. DISCUSSION

A. Fourier modes and sweeping effect

It is tempting to relate the lack of large fluctuations of Fourier modes in the inertial range to their fast decorrelation due to sweeping effect. The idea that the Fourier modes decorrelate faster than predicted by standard cascade arguments has been proposed by Kraichnan in the context of the Direct Interaction Approximation (DIA) [35]. There, it was shown with systematic arguments that the time decorrelation of an inertial Fourier mode $\hat{\vec{u}}(\vec{k},t)$ is of the order of $1/v_0 k$, where v_0 is the rms of velocity fluctuations $\langle u_x^2 \rangle^{1/2}$. There is now almost no doubt that it is effectively the case for true turbulence (see e.g., Ref. [36] and references therein). For the small scales of the real-space velocity field, the sweeping decorrelation is essentially a kinematic effect which can be thought of as a random Galilean transformation [37] (see also Ref. [1], Secs. 6.2.5 and 7.3); the small structures are swept past fixed points almost as a whole by the random energetic large-scale motions, and so there is only little energy redistribution between small and large scales. In Lagrangian coordinates, the sweeping effect is eliminated and the expected turnover time ($\tau \sim r^{2/3}\varepsilon^{-1/3}$) should be (at least approximatively) recovered. But as far as the decorrelation of a given inertial Fourier mode $\hat{\vec{u}}(\vec{k},t)$ is concerned, if one interprets the sweeping effect as being due to rapid *energy exchanges* between the mode $\vec{k}$ and its many neighboring modes $(\vec{k}+\vec{q})$, via the mixing action of the energy containing range $(|\vec{q}| \sim 1/l_0 \ll |\vec{k}|)$, such an approximation leads to improbable large fluctuations for $\hat{\vec{u}}(\vec{k},t)$; the sweeping time $1/v_0 k$ being smaller than the local turnover time of the cascade $\tau \sim \varepsilon^{-1/3} k^{-2/3}$, when $k \to \infty$, the rapid energy mixing may bypass the anomalous cascade fluctuations for the *individual* Fourier modes. Note also that a lateral energy exchange between wave numbers of nearly the same magnitude will not contribute to the energy cascade.

In fact, the above argument is likely to be wrong since there is no need to invoke *energy exchange* between modes to explain their fast decorrelation. We illustrate this point with a random Galilean transformation, following an argument presented in Ref. [38]. Under a Galilean transformation $\vec{x}' = \vec{x} + \vec{V}t$ and $\vec{u}'(\vec{x}',t) = \vec{u}(\vec{x},t) + \vec{V}$, the Fourier modes $\hat{\vec{u}}(\vec{k},t)$ are transformed into $\hat{\vec{u}}'(\vec{k},t) = e^{-i\vec{k}\cdot\vec{V}t}\hat{\vec{u}}(\vec{k},t) + \delta_{\vec{k},\vec{0}}\vec{V}$. Therefore, if $\vec{k} \neq \vec{0}$, we have for the temporal autocorrelation function

$$\langle \hat{\vec{u}}'(\vec{k},0) \cdot \hat{\vec{u}}'(\vec{k},t)^* \rangle = \langle \hat{\vec{u}}(\vec{k},0) \cdot e^{i\vec{k}\cdot\vec{V}t} \hat{\vec{u}}(\vec{k},t)^* \rangle. \quad (4.1)$$

Suppose now that $\vec{V}$ is *random*, characteristic of the large-scale velocity field, and to simplify further suppose $\vec{V}$ is a centered Gaussian vector, independent of the small scales $(k \ll 1/l_0)$. Then

$$\langle \hat{\vec{u}}'(\vec{k},0) \cdot \hat{\vec{u}}'(\vec{k},t)^* \rangle = \langle e^{i\vec{k}\cdot\vec{V}t} \rangle_{\vec{V}} \langle \hat{\vec{u}}(\vec{k},0) \cdot \hat{\vec{u}}(\vec{k},t)^* \rangle_{k \ll 1/l_0} \quad (4.2)$$

$$= e^{-1/2\, k^2 \langle V^2 \rangle t^2} \langle \hat{\vec{u}}(\vec{k},0) \cdot \hat{\vec{u}}(\vec{k},t)^* \rangle_{k \ll 1/l_0}, \quad (4.3)$$

where $\langle \cdot \rangle_{\vec{V}}$ and $\langle \cdot \rangle_{k \ll 1/l_0}$ denote, respectively, the average over the realizations of the $\vec{V}$ process and over the realizations of the small-scale dynamics. If $\langle \hat{\vec{u}}(\vec{k},0) \cdot \hat{\vec{u}}(\vec{k},t)^* \rangle_{k \ll 1/l_0}$ is characteristic of the inertial dynamics, it is then expected to scale with the local turnover time of the cascade, and the whole correlation function is thus dominated by the $\exp(-\frac{1}{2}k^2\langle V^2 \rangle t^2)$ term as $t \to +\infty$. This simple argument suggests that it is the random nature of the phase induced by the large-scale sweeping that is the primary process in the decorrelation of the Fourier modes, so that the sweeping effect has no dynamical link with the weak intermittency of the individual Fourier modes.

B. Fourier modes and shell and tree models

In recent years, the so-called shell models and tree models of turbulence have received considerable interest [39]. In particular, it is well-known that for certain values of its parameters, the Gledzer-Ohkitani-Yamada (GOY) shell model reproduces very well the exponents of the structure functions measured in real flows. These toy models can be regarded as simplified and phenomenological mode decompositions that share the main symmetries and structural properties of the

NS equations. The Fourier representation is indeed only a particular complete functional basis. We discuss briefly some properties of these simplified dynamical models with regard to the influence of the density and type of nonlinear coupling.

The so-called reduced wave-vector set approximation (REWA, see e.g. Ref. [40]) model consits in solving the incompressible NS equations on a geometrically scaling subset $\mathcal{K}$ of wave vectors in Fourier space: $\mathcal{K}=\cup_n \mathcal{K}_n$ with $\mathcal{K}_n = 2^n \mathcal{K}_0$ and $\mathcal{K}_0=\{\pm \vec{k}_0^{\alpha}: \alpha=1,\ldots,N\}$. Each of the wave-vectors shell $\mathcal{K}_n$ represents an octave of wave numbers. The nonlinear term is restricted to neighboring shells, thus local in k space. Numerical simulations showed that the REWA model displays only weak intermittency, whatever the choice of the variables [$\hat{u}(k)$, $\Delta u(r)$, or the shell energy $E_n = \Sigma_{\vec{k}\in\mathcal{K}_n} |\hat{\vec{u}}(\vec{k})|^2$]. This feature has been attributed to the wave-vectors mode representation that does not take into account the scale densification [40]. It has also been observed that increasing the number N of modes in each shell results in weaker intermittency (measurements done for the shell energies) [41]. We propose the following interpretation of this effect, which is also linked with the absence of scale densification. We introduce the short-hand notation: $\vec{k}_n^{\alpha} \equiv 2^n \vec{k}_0^{\alpha}$ and $\hat{\vec{u}}_n^{\alpha} \equiv \hat{\vec{u}}(\vec{k}_n^{\alpha},t)$. Latin superscripts label shells while Greek superscripts label subsystems. The REWA equations may be written under the form:

$$[\partial_t + \nu (k_n^{\alpha})^2]\hat{\vec{u}}_n^{\alpha} = -\Pi(\vec{k}_n^{\alpha}) \circ \sum_{\substack{\beta,\gamma;m,l \\ \vec{k}_n^{\alpha}=\vec{k}_m^{\beta}+\vec{k}_l^{\gamma} \\ |m-n|<R \\ |l-n|<R}} (i\vec{k}_l^{\alpha}\cdot\hat{\vec{u}}_m^{\beta})\hat{\vec{u}}_l^{\gamma}, \tag{4.4}$$

where $\Pi(\vec{k}_n^{\alpha})$ denotes the projector on the plane perpendicular to $\vec{k}_n^{\alpha}$. Thus one may like interpreting the REWA model as describing a set of N subsystems $\vec{u}_{\alpha}(\vec{x},t) \equiv \Sigma_n (e^{i\vec{k}_n^{\alpha}\cdot\vec{x}}\hat{\vec{u}}_n^{\alpha} + \text{c.c.})$ in interaction

$$\partial_t \vec{u}_{\alpha}(\vec{x},t) = \sum_{\beta,\gamma} P_{\alpha}^{R}[(\vec{u}_{\beta}\cdot\vec{\nabla})\vec{u}_{\gamma}] + \nu\nabla^2\vec{u}_{\alpha}(\vec{x},t). \tag{4.5}$$

Let us remark that due to the incompressibility, parallel wave vectors cannot interact, so there are no ''internal'' interactions for any subsystem. Further, since the NS equations are invariant under rotations (for $L\to\infty$), the N directions of space $\pm\vec{k}_0^{\alpha}$, and so the N subsystems, should play approximately the same role for $\mathcal{K}_0$ well chosen. Therefore the nature of the nonlinear energy exchanges in the REWA model is fundamentally different from what happens in NS turbulence, and is rather reminiscent of the spherical shell models introduced by Eyink [42]. A salient feature of shell models is the existence of coherent solitonlike structures that run down the cascade [43,44]. In the case of the spherical shell model studied in Ref. [45], the PDF of the instantaneous exponent of the global energy transfer suggests that pulses transporting anomalous fluctuations are destroyed by ''intersubsystems mixing'' by ''mixing among other subsystems'' when $N\to\infty$, thus restoring K41 scaling in the limit. On the crude level of our analogy, it seems possible that a similar mechanism is at work in the REWA model.

It is worth noting that the same tendency toward a less intermittent regime when increasing the number of coupling has also been observed in the so-called tree models of turbulence [34]. At the difference of the REWA model, the tree models take into account the scale densification. The possible choice of nonlinear interactions are phenomenologically motivated by requiring a certain degree of locality, both in Fourier and real space. Using different sets of nonlinear interactions (conserving energylike and helicitylike quantities), it was shown that the presence of horizontal coupling (i.e., spatial coupling at a given scale) results in a weaker intermittency. In fact, at a given analyzing scale of the turbulent velocity field, the only way energy localization could be avoided is by a strong energy mixing in space [46].

But what is the relationship to the NS equations, where an infinite number of triadic interactions is involved? Our numerical results show that as far as individual Fourier modes are concerned, even when $l_0 \sim L$, only a weak intermittency is observed. This strongly indicates that shell or tree variables should not be assimilated with Fourier modes but are rather akin to wavelets coefficients as originally and usually argued (see e.g., Refs. [47,34]). It is as if, in a statistical sense, simple dynamical models were able to take into account the net effect of complex phase coupling and incompressibility or geometry constraints in k space. Since when $l_0/L\to 0$, the spectral density of modes is increased, and one may want to link the spatial central limit effect for the individual Fourier modes with an increase of nonlinear coupling. Due to the way the Fourier modes become more dense and to the unchanged intermittency of the real-space turbulent fields when $l_0/L\to 0$, the mechanism at work in NS is certainly different than in REWA or tree models. It is just tempting to say that as $l_0/L\to 0$, the fluctuations of an individual Fourier mode is the sum of many excitations, which are nearly statistically independent, see the next section.

One of the major conclusions of this paper is that the statistical properties of the Fourier modes in turbulent flows have nothing to do with the variables used in shell model. The latter are akin to wavelet coefficients, and allow to probe more directly intermittency effects.

C. Multi-k correlations

As inertial Fourier components become individually Gaussian in the limit $l_0/L\to 0$, intermittency should be viewed as a collective phenomena in k space. So one may look at correlators $\langle \hat{u}(\vec{k}_1)\ldots\hat{u}(\vec{k}_p)\rangle$, which appear naturally in Fourier expression of $\langle(\Delta u)^p\rangle$, with the hope of taking into account phase coupling between modes ($\vec{k}_1+\cdots+\vec{k}_p = \vec{0}$ is required when the flow is homogeneous).

We first refer to the ''weak dependence principle'' (WDP) introduced in the context of the DIA [35] in order to discuss qualitatively this issue. Let us briefly recall the weak-

coupling argument due to Kraichnan. Taking cyclic boundary conditions on a box of size L, the incompressible Navier-Stokes equations may be written in the Fourier representation under the form

$$(\partial_t+\nu k^2)\hat{\vec{u}}(\vec{k})=-\Pi(\vec{k})\circ\sum_{\vec{p}+\vec{q}=\vec{k}}[i\vec{k}\cdot\hat{\vec{u}}(\vec{p})]\hat{\vec{u}}(\vec{q}), \quad (4.6)$$

where $\Pi(\vec{k})$ denotes the projector on the plane perpendicular to $\vec{k}$. Consider a wave vector $\vec{k}'$ with $\vec{k}'\neq\pm\vec{k}$, and suppose the statistical dependence between $\hat{\vec{u}}(\vec{k})$ and $\hat{\vec{u}}(\vec{k}')$ being induced wholly by the nonlinear term in (4.6). We see that the wave vector $\vec{k}'$ appears only twice in the convolution, once as $\vec{p}$ and once as $\vec{q}$, thus making a very weak contribution to the sum. As the spectral density of Fourier modes increases when $L\to\infty$, the WDP postulates that the normalized Fourier modes $\hat{\vec{u}}(\vec{k})/\langle|\hat{\vec{u}}(\vec{k})|^2\rangle^{1/2}$ and $\hat{\vec{u}}(\vec{k}')/\langle|\hat{\vec{u}}(\vec{k}')|^2\rangle^{1/2}$ become statistically independent *in the limit* $L\to\infty$ (l_0 is supposed fixed). Note that the WDP does not differentiate the interacting variables on a statistical level, and is defined in terms of a limiting process. In the case of the random coupling model [48], the WDP applied to a finite number of individual variables is an exact result when their total number increases to infinity. But in the case of the NS equations at small but finite l_0/L ratio, due to the influence of intermittency, one may expect the Fourier modes to be correlated with a strength depending on the wave numbers they involve (we shall go back to this point later).

A Fourier mode being a complex quantity, its statistics should be understood as the joint statistics of its real and imaginary parts. In fact, supposing $\hat{\vec{u}}(\vec{k}=\vec{0})=\vec{0}$, $\mathrm{Re}[\hat{\vec{u}}(\vec{k})]$ and $\mathrm{Im}[\hat{\vec{u}}(\vec{k})]$ are not directly connected by the nonlinear term of Eq. (4.6). Invoking the WDP, we infer that their statistical dependence is very weak, infinitely weak in the limit $L\to\infty$ (l_0 fixed). The same reasoning may be applied to the components of the vector $\hat{\vec{u}}(\vec{k})$.

Finally, if in addition we take into account the central limit effect on the individual Fourier modes, we have the conclusion that the joint PDF of $\hat{\vec{u}}(\vec{k})$ and $\hat{\vec{u}}(\vec{k}')$ becomes Gaussian in the limit $l_0/L\to0$, as the product of univariate PDF's of independent Gaussian random variables. The above arguments apply by extension to any *finite* number of modes. Even when $l_0\sim L$, based on our numerical results on the univariate statistics of Fourier modes and due to the huge number of modes in interaction, we expect that inertial multivariate statistics of a finite number of Fourier modes could only be close to Gaussian in turbulent homogeneous flows at finite Reynolds number. However, we expect the difference with Gaussianity to increase with the scales.

The WDP is in agreement with an approach based on a r-space cumulant expansion of $\langle\hat{u}(\vec{k}_1)\ldots\hat{u}(\vec{k}_p)\rangle$. For simplicity, we consider the case $p=4$. We denote $\hat{u}(\vec{k})$ a component of the vector $\hat{\vec{u}}(\vec{k})$. It is straightforward to show that

$$\begin{aligned}\langle\hat{u}(\vec{k}_1)\hat{u}(\vec{k}_2)\hat{u}(\vec{k}_3)\hat{u}(\vec{k}_4)\rangle&=\delta_{\vec{k}_1+\vec{k}_2}\delta_{\vec{k}_3+\vec{k}_4}\langle\hat{u}(k_1)\hat{u}(k_2)\rangle\langle\hat{u}(k_3)\hat{u}(k_4)\rangle\\&+\delta_{\vec{k}_1+\vec{k}_3}\delta_{\vec{k}_2+\vec{k}_4}\langle\hat{u}(k_1)\hat{u}(k_3)\rangle\langle\hat{u}(k_2)\hat{u}(k_4)\rangle\\&+\delta_{\vec{k}_1+\vec{k}_4}\delta_{\vec{k}_2+\vec{k}_3}\langle\hat{u}(k_1)\hat{u}(k_4)\rangle\langle\hat{u}(k_2)\hat{u}(k_3)\rangle\\&+\epsilon(\vec{k}_1,\vec{k}_2,\vec{k}_3,\vec{k}_4),\end{aligned} \quad (4.7)$$

where

$$\begin{aligned}&\epsilon(\vec{k}_1,\vec{k}_2,\vec{k}_3,\vec{k}_4)\\&\equiv\frac{1}{L^{12}}\int\int\int\int d^3x_1\,d^3x_2\,d^3x_3\,d^3x_4\\&\times e^{-i(\vec{k}_1\cdot\vec{x}_1+\cdots+\vec{k}_4\cdot\vec{x}_4)}\langle u(\vec{x}_1)u(\vec{x}_2)u(\vec{x}_3)u(\vec{x}_4)\rangle_c,\end{aligned} \quad (4.8)$$

and $\langle u(\vec{x}_1)u(\vec{x}_2)u(\vec{x}_3)(\vec{x}_4)\rangle_c$ is the cumulant of $\langle u(\vec{x}_1)u(\vec{x}_2)u(\vec{x}_3)u(\vec{x}_4)\rangle$. If l_0 is kept fixed, one infers that [18]

$$\epsilon(\vec{k}_1,\vec{k}_2,\vec{k}_3,\vec{k}_4)/\mathcal{N}(\vec{k}_1,\vec{k}_2,\vec{k}_3,\vec{k}_4)\to0 \quad \text{as} \quad L\to\infty, \quad (4.9)$$

where

$$\begin{aligned}&\mathcal{N}(\vec{k}_1,\vec{k}_2,\vec{k}_3,\vec{k}_4)\\&\equiv\langle|\hat{u}(\vec{k}_1)|^2\rangle^{1/2}\langle|\hat{u}(\vec{k}_2)|^2\rangle^{1/2}\langle|\hat{u}(\vec{k}_3)|^2\rangle^{1/2}\langle|\hat{u}(\vec{k}_4)|^2\rangle^{1/2}.\end{aligned} \quad (4.10)$$

The WDP applied to $\langle\hat{u}(\vec{k}_1)\hat{u}(\vec{k}_2)\hat{u}(\vec{k}_3)\hat{u}(\vec{k}_4)\rangle/\mathcal{N}(\vec{k}_1,\vec{k}_2,\vec{k}_3,\vec{k}_4)$ leads directly to the same result, except when the correlation $\langle\hat{u}(\vec{k}_1)\hat{u}(\vec{k}_2)\hat{u}(\vec{k}_3)\hat{u}(\vec{k}_4)\rangle$ collapses in the fourth moment of a *single* mode, $\langle|\hat{u}(\vec{k})|^4\rangle$.

Since $\langle\Delta u(\vec{r})^4\rangle$ has an anomalous scaling behavior, and

$$\begin{aligned}\langle\Delta u(\vec{r})^4\rangle&=\sum_{\vec{k}_1+\vec{k}_2+\vec{k}_3+\vec{k}_4=\vec{0}}(e^{i\vec{k}_1\cdot\vec{r}}-1)\\&\times\cdots\times(e^{i\vec{k}_4\cdot\vec{r}}-1)\,\langle\hat{u}(\vec{k}_1)\hat{u}(\vec{k}_2)\hat{u}(\vec{k}_3)\hat{u}(\vec{k}_4)\rangle\end{aligned} \quad (4.11)$$

$$\begin{aligned}&=3\langle\Delta u(r)^2\rangle^2+\sum_{\vec{k}_1+\vec{k}_2+\vec{k}_3+\vec{k}_4=\vec{0}}(e^{i\vec{k}_1\cdot\vec{r}}-1)\\&\times\cdots\times(e^{i\vec{k}_4\cdot\vec{r}}-1)\,\epsilon(\vec{k}_1,\vec{k}_2,\vec{k}_3,\vec{k}_4),\end{aligned} \quad (4.12)$$

the $\epsilon(\vec{k}_1,\vec{k}_2,\vec{k}_3,\vec{k}_4)$ term has to embody the anomalous scaling. What is unclear to us is whether this scaling depends on the geometry of the $\vec{k}_j$. For instance, when $\vec{k}_1=-\vec{k}_2=\vec{k}_3=-\vec{k}_4=\vec{k}$, Eq. (4.7) degenerates into

$$\langle|\hat{u}(\vec{k})|^4\rangle=2\langle|\hat{u}(\vec{k})|^2\rangle^2+\epsilon(\vec{k},-\vec{k},\vec{k},-\vec{k}). \quad (4.13)$$

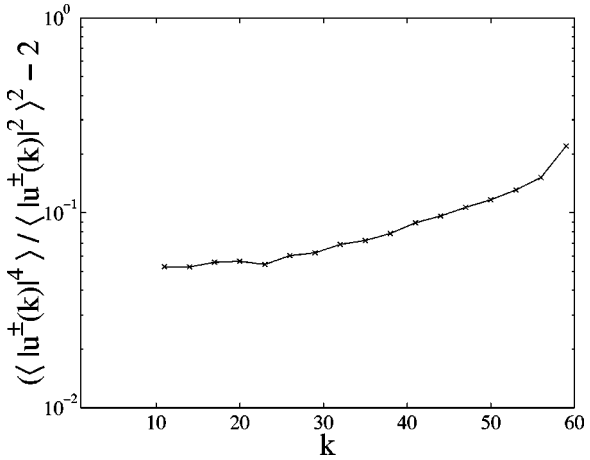

FIG. 6. $\langle|\hat{u}^{\pm}(k)|^4\rangle/\langle|\hat{u}^{\pm}(k)|^2\rangle^2-2$ vs k in semilogarithmic coordinates for our run NS3 ($R_\lambda \sim 80$).

If $\epsilon(\vec{k},-\vec{k},\vec{k},-\vec{k})$ has an anomalous scaling, it should be observable on $\langle|\hat{u}(\vec{k})|^4\rangle/\langle|\hat{u}(\vec{k})|^2\rangle^2$ as $k\to\infty$, in an *infinite* Reynolds number situation. Observe that this does not occur in the simple synthetic wavelet cascade we considered in Sec. IV. For our NS simulation at $R_\lambda \sim 80$ (run NS3), we present in Fig. 6 the behavior of $\langle|\hat{u}(\vec{k})|^4\rangle/\langle|\hat{u}(\vec{k})|^2\rangle^2-2$ vs k in semilog coordinates. We observe a slight increase, close to an exponential behavior.

Last, assuming the presence of an anomalous scaling in a fixed not degenerated $(\vec{k}_j)_{1\leqslant j\leqslant 4}$ geometry ($\vec{k}_1+\vec{k}_2+\vec{k}_3+\vec{k}_4=\vec{0}$ and $\vec{k}_i\neq\pm\vec{k}_j$), we have

$$\frac{\langle\hat{u}(\lambda\vec{k}_1)\hat{u}(\lambda\vec{k}_2)\hat{u}(\lambda\vec{k}_3)\hat{u}(\lambda\vec{k}_4)\rangle}{\langle|\hat{u}(\lambda\vec{k}_1)|^2\rangle^{1/2}\langle|\hat{u}(\lambda\vec{k}_2)|^2\rangle^{1/2}\langle|\hat{u}(\lambda\vec{k}_3)|^2\rangle^{1/2}\langle|\hat{u}(\lambda\vec{k}_4)|^2\rangle^{1/2}} \to\infty \quad \text{as} \quad \lambda\to\infty. \tag{4.14}$$

We recall that if the $\hat{u}(\vec{k}_j)$ are independent, then the correlation $\langle\hat{u}(\lambda\vec{k}_1)\hat{u}(\lambda\vec{k}_2)\hat{u}(\lambda\vec{k}_3)\hat{u}(\lambda\vec{k}_4)\rangle$ is zero due to the spatial homogeneity. Equation (4.14) means that the intermittency effects lead to a stronger and stronger correlation of the Fourier modes, as the wave number k increases.

N-points real-space statistics contain indeed the correlations among Fourier modes and are easier to handle experimentaly or analytically. We note that in the context of the weak wave turbulence theory [49], a (k,ω) formalism is explicitely involved, and a joint Gaussian approximation is used to derive the so-called Kolmogorov-Zakharov finite flux solutions. In order to test the validity of the latter approximation, some kinds of real-space structure functions seem to us better suited than univariate k-space statistical tests like in Ref. [50].

V. CONCLUSION

The main result of this paper is to show by DNS that even when $l_0\sim L$, the individual Fourier modes are only weakly intermittent at high enough Reynolds numbers. Our results are in qualitative agreement with recent ultrasound scattering experiments [10], but disagree with the numerical results obtained in Ref. [19].

Using a simple model of cascade defined on a dyadic structure [28], we illustrated how a spatial decorrelation process through the inertial scales may explain the weak inertial intermittency of the $\hat{u}(k)$; in true turbulent dynamics, we expect this decorrelation process to breakdown in the dissipation range, thus allowing the known dissipative intermittency of the $\hat{u}(k)$ as $k\eta\to\infty$.

We then addressed our results on a more general ground. We discussed our findings with regard to the temporal autocorrelation function of the $\hat{u}(k)$, and also with regard to some simplified mode decomposition approaches to turbulence. Last, we discussed k-space inertial multivariate statistics, with arguments indicating that the latter is also plagued by an influence of the l_0/L ratio.

ACKNOWLEDGMENTS

We acknowledge J. F. Pinton and S. Fauve for very stimulating discussions. We gratefully thank ''IDRIS,'' Paris, for computer resources. The financial support from the EU, under Contract No. FMRX-CT98-0175, is also acknowledged.

[1] U. Frisch, *Turbulence: The Legacy of AN Kolmogorov* (Cambridge University, Cambridge, 1995).
[2] M. Nelkin, Adv. Phys. **43**, 143 (1994).
[3] K. R. Sreenivasan and R. A. Antonia, Annu. Rev. Fluid Mech. **29**, 435 (1997).
[4] F. Anselmet, Y. Gagne, E. Hopfinger, and R. A. Antonia, J. Fluid Mech. **140**, 63 (1984).
[5] R. A. Antonia, E. J. Hopfinger, Y. Gagne, and F. Anselmet, Phys. Rev. A **30**, 2704 (1984).
[6] A. N. Kolmogorov, Dokl. Akad. Nauk (SSSR) **30**, 299 (1941) [Sov. Phys. Dokl. **10**, 734 (1968)].
[7] M. Chertkov *et al.*, Phys. Rev. E **52**, 4924 (1995).
[8] K. Gawędzki and A. Kupiainen, Phys. Rev. Lett. **75**, 3834 (1995).
[9] B. I. Shraiman and E. D. Siggia, C. R. Acad. Sci., Ser. IIb: Mec., Phys., Chim., Astron. **321**, 279 (1995).
[10] A. Petrossian and J.-F. Pinton, J. Phys. II **7**, 801 (1997).
[11] D. C. Leslie, *Developments in the Theory of Turbulence* (Clarendon, Oxford, 1973).
[12] W. D. McComb, *The Physics of Fluid Turbulence* (Oxford University, Oxford, 1990).
[13] T. D. Lee, J. Appl. Math. Mech. **10**, 69 (1952).
[14] S. A. Orszag, ''Lectures on the Statistical Theory of Turbulence'' in *Fluids Dynamics 1973, Les Houches Summer School of Theoretical Physics*, edited by R. Balian and J. L. Peube (Gordon and Breach, New York, 1977).
[15] J. Lumley, in *Statistical Models and Turbulence*, edited by M.

Rosemblatt and C. Van Atta (Springer-Verlage, New York, 1972), pp. 1–26.
[16] A. V. Ivanov and N. N. Leonenko, *Statistical Analysis of Random Fields* (Kluwer Academic, Dordrecht, 1989).
[17] Z. Fan and J. M. Bardeen, Phys. Rev. D **51**, 6714 (1995).
[18] A. Pumir, J. Phys. (Paris) **46**, 511 (1985).
[19] S. K. Dhar, A. Sain, and R. Pandit, Phys. Rev. Lett. **78**, 2964 (1997).
[20] A. Pumir, Phys. Fluids **6**, 2118 (1994).
[21] V. Borue and S. A. Orszag, Europhys. Lett. **29**, 687 (1995).
[22] G. K. Batchelor and A. A. Townsend, Proc. R. Soc. London, Ser. A **199**, 238 (1949).
[23] R. H. Kraichnan, Phys. Fluids **10**, 2080 (1967).
[24] S. Chen, G. Doolen, J. R. Herring, R. H. Kraichnan, S. A. Orszag, and Z. S. She, Phys. Rev. Lett. **70**, 3051 (1993).
[25] U. Frisch and R. Morf, Phys. Rev. A **23**, 2673 (1981).
[26] F. Okkels and M. H. Jensen, Phys. Rev. E **57**, 6643 (1998).
[27] J.-F. Pinton, private communication.
[28] R. Benzi, L. Biferale, A. Crisanti, G. Paladin, M. Vergassola, and A. Vulpiani, Physica D **65**, 352 (1993).
[29] P. Olla and P. Paradisi, Physica D (to be published); Los Alamos preprint chao-dyn/9803039.
[30] A. Arneodo, E. Bacry, S. Manneville, and J. F. Muzy, Phys. Rev. Lett. **80**, 708 (1998).
[31] W. Press, S. Teukolsky, W. Vetterling, and B. Flannery, *Numerical Recipes in Fortran* (Cambridge University, Cambridge, 1992).
[32] S. G. Mallat, IEEE Trans. Pattern Anal. Mach. Intell. **11**, 674 (1989).
[33] I. Daubechies, Commun. Pure Appl. Math. **41**, 909 (1988).
[34] R. Benzi, L. Biferale, R. Tripiccione, and E. Trovatore, Phys. Fluids **9**, 2355 (1997).
[35] R. H. Kraichnan, J. Fluid Mech. **5**, 497 (1959).
[36] T. Sanada and V. Shanmugasundaram, Phys. Fluids A **4**, 1245 (1992).
[37] R. H. Kraichnan, Phys. Fluids **7**, 1030 (1964).
[38] V. Yakhot, S. A. Orszag, and Z.-S. She, Phys. Fluids A **1**, 184 (1989).
[39] T. Bohr, M. H. Jensen, G. Paladin, and A. Vulpiani, *Dynamical Systems Approach to Turbulence and Extended Systems* (Cambridge University Press, Cambridge, England, 1998).
[40] S. Grossmann, D. Lohse, and A. Reeh, Phys. Rev. Lett. **77**, 5369 (1996).
[41] C. Uhlig and J. Eggers, Z. Phys. B: Condens. Matter **102**, 513 (1997).
[42] G. L. Eyink, Phys. Rev. E **49**, 3990 (1994).
[43] E. D. Siggia, Phys. Rev. A **17**, 1166 (1978).
[44] T. Dombre and J.-L. Gilson, Physica D **111**, 265 (1998); J.-L. Gilson and T. Dombre, Phys. Rev. Lett. **79**, 5002 (1997).
[45] D. Pierotti, Europhys. Lett. **37**, 323 (1997).
[46] R. H. Kraichnan, J. Fluid Mech. **62**, 305 (1974).
[47] E. D. Siggia, Phys. Rev. A **15**, 1730 (1977).
[48] R. H. Kraichnan, J. Math. Phys. **2**, 124 (1961).
[49] V. E. Zakharov, V. S. L'vov, and G. E. Falkovich, *Kolmogorov Spectra of Turbulence* (Springer-Verlag, New York, 1992).
[50] A. J. Majda, D. W. MacLaughlin, and E. C. Tabak, J. Nonlinear Sci. **6**, 9 (1997).